The Insulin-Like Growth Factor-I Receptor Inhibitor Picropodophyllin Causes Tumor Regression and Attenuates Mechanisms Involved in Invasion of Uveal Melanoma Cells

Ada Girnita,[1] Charlotta All-Ericsson,[2] Mario A. Economou,[2] Kristina Åström,[1] Magnus Axelson,[3] Stefan Seregard,[2] Olle Larsson,[1] and Leonard Girnita[1]

Abstract

Purpose: Uveal melanoma has a high mortality rate due to a high incidence of metastasis (up to 50%), which preferentially occurs in the liver. Conventional chemotherapy, being the only therapeutic option today against metastatic uveal melanoma, has not proved to be effective. Therefore, new molecular targets important for malignant phenotype of uveal melanoma have to be found to design efficient pharmacologic agents.

Experimental Design: We previously reported data indicating that the insulin-like growth factor-1 receptor (IGF-IR) is a metastasis predictor as well as a therapeutic target for uveal melanoma. In the present study, we made use of the cyclolignan picropodophyllin (PPP), which is an inhibitor of the IGF-IR.

Results: We showed that PPP efficiently blocks growth and viability of uveal melanoma cells in cultures and causes tumor regression in xenografted mice. In addition, treatment with PPP inhibited several mechanisms involved in metastasis, including tumor cell adhesion to extracellular matrix proteins, activity and expression of matrix metalloproteinase 2, and cell migration as well as invasion through basement membranes and endothelial cell layers. Furthermore, PPP significantly delayed establishment of uveal melanoma tumors and drastically reduced the incidence of liver metastasis in mice.

Conclusions: Our data suggest that IGF-IR is crucial for growth and survival as well as invasion and metastasis of uveal melanoma cells. Targeting this receptor may therefore comprise a strategy to treat ongoing disease (today incurable) as well as a strategy to prevent development of metastases in patients with primary disease.

Uveal melanoma is the most common primary intraocular malignant tumor in adults. It has an elevated mortality rate due to a high incidence of metastases, which occur preferentially in the liver (1, 2). The treatment regimen today is enucleation or radiation of the primary tumor. There are no postoperative adjuvant therapies available to decrease the risk of metastasis and treatment against metastatic uveal melanoma has not been effective. Therefore, new molecular targets need to be established to provide effective treatment modalities.

In uveal melanoma, metastasis is the crucial event determining the outcome of patients. Search for agents decreasing the metastatic potential of the primary tumor is therefore of particular interest. Metastasis is a process involving many components, including tumor cell adhesion, migration, extracellular matrix (ECM) proteolysis, and invasion. The tumor cells undergo intravasation, disperse via the vascular and the lymphatic systems, and finally extravasate to invade the secondary sites. In all these steps, proteolytic enzyme systems are involved, including the matrix metalloproteinase (MMP) system and the plasminogen activation system. The migration of a malignant cell through the ECM and the basement membrane requires proteolytic activities (3). Baker et al. (4) have shown that uveal melanomas express both MMP-2 and MMP-9, tissue inhibitor of metalloproteases 2, urokinase plasminogen activator, plasminogen activator inhibitor 1 and 2, as well as different integrins.

The preferential dissemination to the liver raises the possibility that hepatic environmental factors are important for the growth and progression of uveal melanoma. Such conditions may involve growth factors produced in the liver [e.g., insulin-like growth factor 1 (IGF-I) serving as a ligand of the IGF-I receptor (IGF-IR)]. Ligand binding to the IGF-IR activates the intrinsic tyrosine kinase of the β-subunit leading to phosphorylation of IGF-IR, which in turn activates key signal transduction molecules involved in cell proliferation and

apoptosis protection, such as the mitogen-activated protein kinases and the phosphoinositol-3-kinase (5–8).

Efforts to target IGF-I system in melanoma in the past have been made (9–12). Recently, we detected expression of IGF-IR in clinical samples of uveal melanoma and showed that cultured uveal melanoma cells responded to inhibition of IGF-IR (using, e.g., neutralizing antibodies) by cell death (13). These data pointed to the possibility of using IGF-IR as target for uveal melanoma. Recently, we showed that the cyclolignan picropodophyllin (PPP) acts as a specific inhibitor of the IGF-IR tyrosine phosphorylation without inhibiting the highly homologous insulin receptor (14–18). PPP was proved to also inhibit phosphorylation of IGF-IR in tumor tissues of xenografted mice and phosphorylation of downstream signaling molecules [extracellular signal-regulated kinase (ERK) and Akt] was decreased (14). Subsequently, the tumor cell xenografts underwent complete regression.

In this study, we aimed to investigate the effects of PPP on uveal melanoma cell cultures and xenografts with special focus on mechanisms important for tumor cell invasion.

Materials and Methods

Reagents. PPP was synthesized as described (14) and was dissolved in DMSO (0.5 mmol/L) before addition to cell cultures. The phosphotyrosine (PY99) and polyclonal antibodies to the β-subunit of IGF-IR (H-60) were from Santa Cruz Biotechnology, Inc. (Santa Cruz, CA).

Cell cultures. Three cell lines obtained from human primary uveal melanomas (OCM-1, OCM-3, and 92-1) were previously described (13). R+ cells (overexpressing the human IGF-IR) were from Dr. Renato Baserga (Thomas Jefferson University, Philadelphia, PA). R+ cell line was cultured in the presence of G-418 (Promega, Madison, WI).

Immunoprecipitation and Western blotting. Cells were cultured to subconfluency in 6-cm plates. After indicated treatments, cells were analyzed for IGF-IR, ERK1/2, and Akt phosphorylation as described elsewhere (19, 20).

Cell survival assay. Cell viability determinations were done using the Cell Proliferation Kit II (Roche, Inc., Indianapolis, IN), which is based on colorimetric change of the yellow tetrazolium salt 2,3-bis[2-methoxy-4-nitro-5-sulfophenyl]-2H-tetrazolium-5-carboxanilide inner salt in orange formazan dye by the respiratory chain of viable cells (21).

Integrin expression profile. Expression profile of collagen-specific integrins ($α_1$, $α_2$, $α_3$, $α_v$, $β_1$, $β_3$, and $α_vβ_3$) was assessed by fluorescence-activated cell sorting using antibodies in the Chemicon Investigator Kit (Chemicon Europe, Hampshire, United Kingdom).

ECM adhesion assays. Adhesion of uveal melanoma cells to ECM proteins (collagen type I, collagen type IV, fibronectin, laminin, and vitronectin) was assessed using a CytoMatrix screening kit (Chemicon International, Temecula, CA) following the protocol of the manufacturer. Cells were nonenzymatically disaggregated from culture flasks using cell dissociation solution (Sigma-Aldrich, Stockholm, Sweden) and resuspended at a concentration of $5 × 10^5$/mL in RPMI 1640 with 0.1% bovine serum albumin. Cell suspension (100 μL) was added to each well and the plate was incubated at 37°C for 1 hour. After washings and staining (0.2% crystal violet in 10% ethanol for 5 minutes), the levels of adhesion were determined by measuring the absorbance at 540 nm on a microplate reader. Triplicate wells were assessed for each treatment; experiments were repeated thrice and the mean value was calculated. In all cases, adhesion to wells coated with bovine serum albumin acted as negative controls and levels of adhesion to ECM substrates were calculated relatively to the controls.

Gelatin zymography. The gelatinolytic activity of MMP-2 was analyzed by zymography as previously described (22). Unheated aliquots of conditioned media (50× concentrated) were electrophoresed on a 7.5% SDS polyacrylamide gel containing 1 mg/mL gelatin (Bio-Rad, Stockholm, Sweden) before and after 2-hour treatment with the MMP-2 activator *p*-aminophenylmercuric acetate (APMA; 1 mmol/L). Recombinant MMP-2 (Chemicon International) was used as control. Molecular weight standards were run simultaneously. The gels were stained with Coomassie blue and destained with acetic acid-methanol until the desired color intensity was obtained. Gelatinolytic enzymes were detected as transparent bands on the background of Coomassie blue–stained gelatin.

Assessment of cell migration and invasion in vitro. To assay the effect of PPP on migration and invasion of uveal melanoma cells, BD BioCoat Matrigel chambers were used following the instructions of the manufacturer (BD Biosciences, San Diego, CA). In brief, cells ($5 × 10^4$/mL) treated with PPP or solvent for 1 hour were washed and put into chambers containing an 8-μm pore size PET membrane without (for assay of migration) or with a thin layer of Matrigel serving as a reconstituted basement membrane (for assay of basement membrane invasion) or with basement membrane covered by confluent human endothelial human umbilical vascular endothelial cells (for assay of endothelial invasion) for overnight incubation (23). Medium containing 10% serum or IGF-I (as a chemoattractant) is added to the well outside of the chambers.

In vivo *experiments.* Ten-week-old pathogen-free severe combined immunodeficient mice were used and housed within plastic isolators in a sterile facility. OCM-1 cells were injected s.c. at 10^7 cells per mice in a 0.2-mL volume of sterile saline solution. Experimental treatments with PPP were done as we previously described (14). All of the experiments were done according to the ethical guidelines for laboratory animal use and approved by the institutional ethical committee.

Experimental reproducibility. All experiments were repeated at least thrice with similar results.

Results

Effects of PPP on IGF-IR phosphorylation and survival of uveal melanoma cells. We analyzed phosphorylation of IGF-IR in cultured uveal melanoma cells stimulated with IGF-I as well as the dose-response effects of PPP on IGF-IR phosphorylation in these systems. OCM-1 and 92-1 cells had first been serum depleted overnight and then treated with solvent (negative control) or PPP for 60 minutes at various concentrations and finally stimulated with IGF-I for 5 minutes, which is the stimulation time for maximal IGF-IR phosphorylation (15). Both cell lines responded with a clear IGF-IR activation (Fig. 1A). Consistent with results obtained from several other cell types (14, 15, 18), PPP dose-dependently reduced IGF-I-induced receptor phosphorylation (Fig. 1A). In contrast, the IGF-IR expression was not affected by this short treatment with PPP (Fig. 1A). As assessed by densitometry, 500 nmol/L PPP reduced the level of IGF-IR phosphorylation by >50% (data not shown). The PPP treatment also led to decreased phosphorylation of the downstream molecules Akt and ERK1/2 (Fig. 1B).

Next, we investigated the effects of PPP on survival of cultured uveal melanoma cells. The cells were treated with different concentrations of PPP for 48 hours. Cell survival was assessed by 2,3-bis[2-methoxy-4-nitro-5-sulfophenyl]-2H-tetrazolium-5-carboxanilide inner salt. Figure 1C shows that the IGF-IR inhibitor efficiently decreased viability of the three studied cell lines (OCM-1, OCM-3 and 92-1). A PPP concentration of 500 nmol/L reduced cell survival by 60% to 90%. Consistent with the effects on IGF-IR phosphorylation, the IC_{50} values are between 50 and 500 nmol/L (Fig. 1C). We also analyzed the effects of IGF-I on viability of uveal

melanoma cells. OCM-1 cells were serum depleted with and without IGF-I over a 48-hour period. The presence of IGF-I drastically increased viability of the serum-depleted cells (Fig. 1D). However, if PPP (500 nmol/L) was present, this effect of IGF-I was completely abrogated (Fig. 1D).

Effects of PPP on invasion mechanisms in vitro. Invasion involves several crucial mechanisms. One early step is cell adhesion (through integrins at the cell surface) to ECM components. It was recently shown that α_1, α_2, and α_3 integrins showed higher expression in uveal melanoma cells with invasive phenotype compared with noninvasive cells, and inhibition of these α integrins decreased binding to collagen IV, fibronectin, and laminin (24). This is interesting because these three ECM proteins have been reported to surround the

tumor cells in primary and metastatic uveal melanomas (25). We first investigated the expression profiles of collagen-specific integrins in OCM-1 and OCM-3. Interestingly, both cell lines expressed fully detectable to high amounts of α_1, α_2, and α_3 integrins (Fig. 2A). Because IGF-IR has previously been shown to control integrin-mediated cell adhesion to ECM proteins (26), we next analyzed the effects of PPP on uveal melanoma cell adhesion to collagen type IV, fibronectin, and laminin in comparison with collagen type I and vitronectin. The cells were treated for 1 hour with three different concentrations of PPP (0, 50, and 500 nmol/L). In a separate experiment, it was shown that 1-hour treatment with PPP does not decrease cell survival (data not shown). PPP induced a strong dose-dependent inhibition of adhesion to fibronectin, laminin,

Fig. 1. Effects of PPP on phosphorylation of IGF-IR and growth of uveal melanoma cells. *A,* cultured OCM-1 and 92-1 cells were serum depleted overnight and then treated with PPP at the indicated concentrations (0-2,500 nmol/L) for 1 hour. IGF-I was then added for a 5-minute incubation, whereupon cells were harvested for immunoprecipitation of IGF-IR. The immunoprecipitates were fractionated by gel electrophoresis and then immunoblotted with a phosphotyrosine antibody or an antibody to the β-subunit of the IGF-IR (loading control). *B,* OCM-1 cells were serum depleted overnight and then treated with PPP at the indicated concentrations (0-2,500 nmol/L) for 1 hour. IGF-I was then added for a 5-minute incubation. The cell lysates were analyzed for pAkt/Akt and pERK1/2/ERK1/2. *C,* cultured OCM-1, OCM-3, and 92-1 cells were cultured in complete medium containing 10% serum in 96-well plates. When the cells had reached subconfluency, they were treated with PPP at the indicated concentrations (50-2,500 nmol/L) for 48 hours. Cells were assayed for viability using the 2,3-bis[2-methoxy-4-nitro-5-sulfophenyl]-2*H*-tetrazolium-5-carboxanilide inner salt assay. Points, mean of triplicates; bars, SD. *D,* OCM-1 cells were serum depleted with or without IGF-I (100 ng/mL). The effects of PPP (500 nmol/L) on unstimulated and IGF-I stimulated cells were also investigated. After incubation for 48 hours, cell viability was assayed by 2,3-bis[2-methoxy-4-nitro-5-sulfophenyl]-2*H*-tetrazolium-5-carboxanilide inner salt. Columns, mean of triplicates; bars, SD.
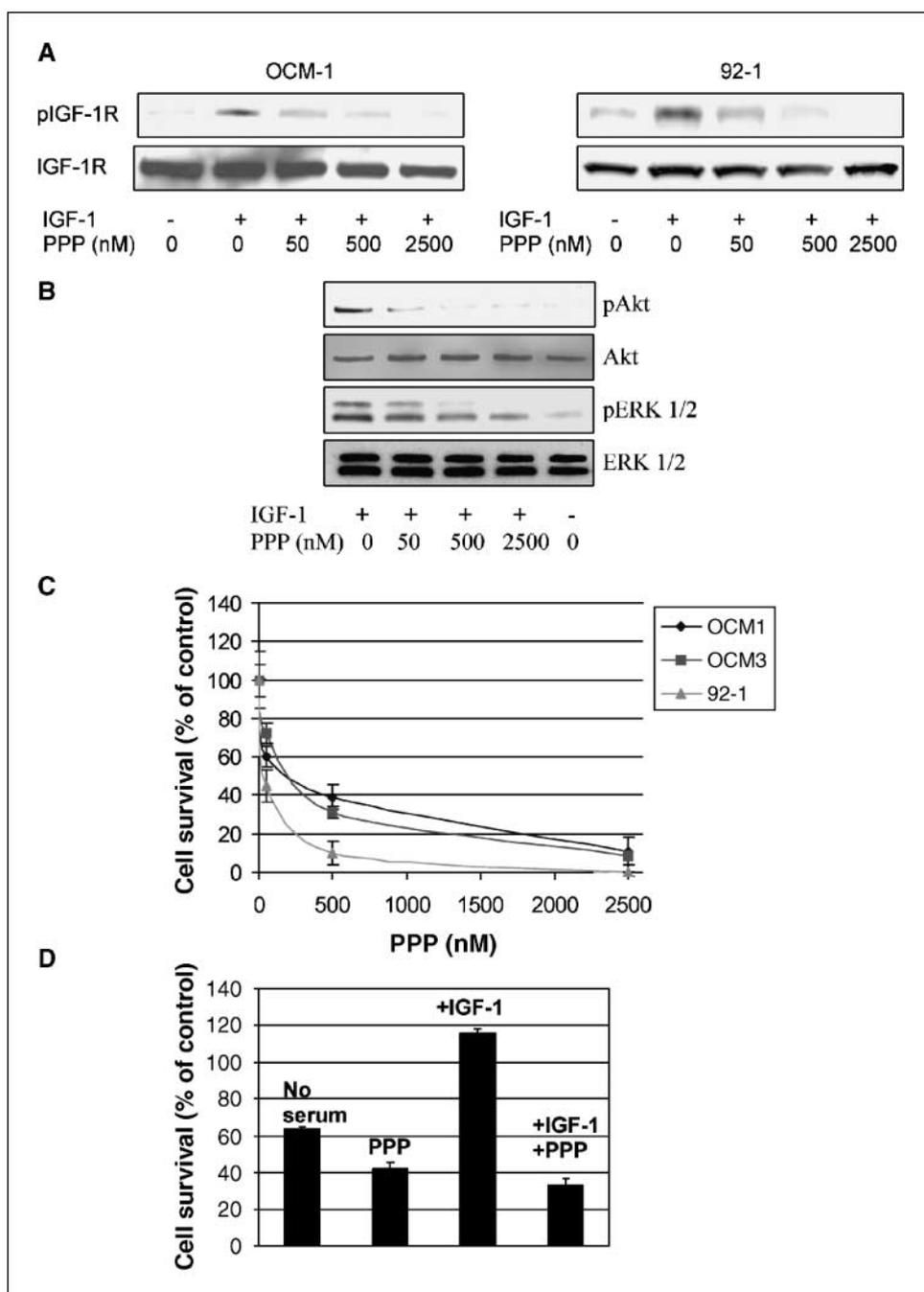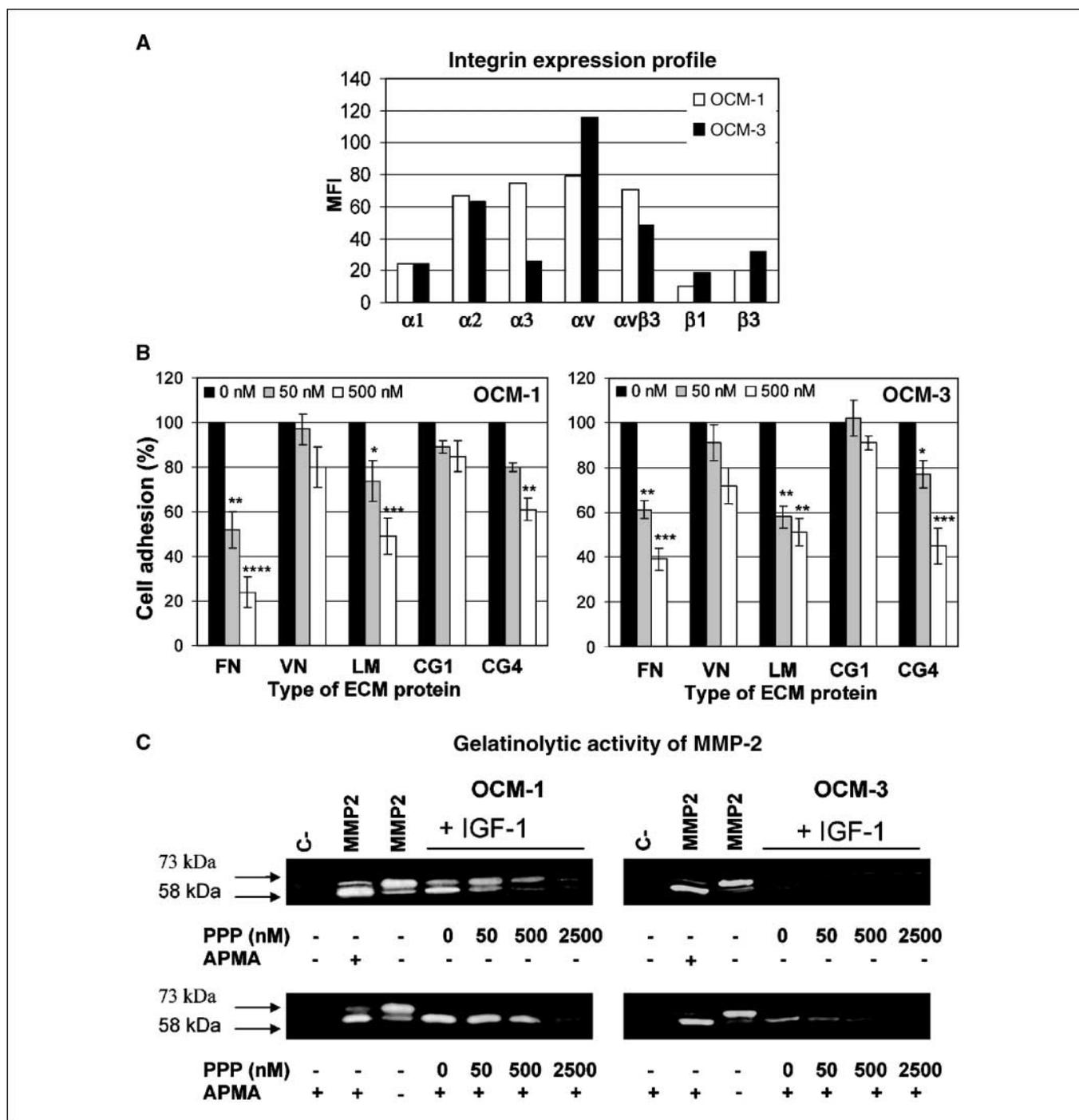
Fig. 2. Effect of PPP on uveal melanoma cell adhesion. *A,* OCM-1 and OCM-3 cells were analyzed for expression profile of collagen-specific integrins using the CHEMICON kit. *B,* OCM-1 and OCM-3 were cultured in 96-well plates precoated with fibronectin (*FN*), vitronectin (*VN*), laminin (*LM*), collagen type I (*CG1*), or collagen type IV (*CG4*). The cells were treated for 1 hour with two different concentrations of PPP (50 and 500 nmol/L) or were left untreated. *, $P < 0.05$; **, $P < 0.01$; ***, $P < 0.005$; ****, $P < 0.001$. The effects on cell adhesion of these ECM proteins were determined as described in Materials and Methods. Columns, mean; bars, SD. *C,* OCM-1 and OCM-3 cells were serum depleted overnight and then treated with IGF-I (10 ng/mL) and different concentrations (0, 50, 500, and 2,500 nmol/L) of PPP for 6 hours. The negative control (*C-*) was treated with IGF-I and PPP. The conditioned media were collected and treated with the MMP-2 activator APMA (1 mmol/L; *bottom*) or remained untreated (*top*). As negative control (*C-*), cells were incubated with serum-free medium without IGF-I. Activated and inactivated recombinant MMP-2 were used as positive controls. The gelatinolytic activity of MMP-2 in the conditioned media was detected as transparent bands on the background of Coomassie blue–stained gelatin.

and collagen IV (Fig. 2B). Vitronectin and collagen I, on the other hand, were not significantly affected.

MMP-2 is generally a required for invasive and metastatic capability of malignant cells and has been suggested to be controlled by the IGF-I signaling (22). Therefore, we investigated the effect of IGF-I stimulation on gelatinolytic activity of MMP-2 secreted from uveal melanoma cells and whether PPP could interfere with this event. OCM-1 and OCM-3 cells were incubated in serum-free medium with and without IGF-I and PPP at different concentrations for 6 hours. It was confirmed

that 6-hour treatment with PPP does not significantly decrease cell survival (data not shown). The conditioned media were collected and treated with APMA (an MMP-2 activator) or untreated before electrophoresis. Recombinant MMP-2, activated or not by APMA, was used as control. Accordingly, gelatin zymography revealed two bands corresponding to the native (72-kDa) and activated (62-kDa) forms of MMP-2 (Fig. 2C). No MMP-2 expression was seen in cells that were not stimulated with IGF-I (C-). In the presence of IGF-I but in the absence of APMA, both the native and active MMP-2 appeared (Fig. 2C, top). PPP decreased in a dose-dependent manner the amount of active MMP-2 (Fig. 2C, top). In APMA-treated samples, only the active MMP-2 was seen after IGF-I stimulation and was dose-dependently decreased by PPP (Fig. 2C, bottom). Taken together, these data suggest that both the IGF-I-induced activation and expression of MMP-2 are repressed by PPP.

Next, we investigated whether PPP could affect migration of uveal melanoma cells *in vitro* using matrix chambers containing a pored membrane using 10% serum as a chemoattractant (27, 28). Cells were incubated only with solvent or with PPP (50 or 500 nmol/L) for 1 hour and then added to the chambers overnight. It was confirmed that 1-hour treatment with PPP did not lead to reduced cell viability (data not shown). Figure 3A (left) shows that 100% of both OCM-1 and OCM-3 control cells had migrated through the membrane. However, after treatment with 50 and 500 nmol/L PPP, only 55% to 65% and 15% to 20% of the uveal melanoma cells, respectively, could pass the membrane (Fig. 3A). These responses are also illustrated by the microphotographs in Fig. 3A (right). The results imply that PPP efficiently reduces cell migration.

By adding a reconstituted basement membrane on the pored membrane, we repeated the experiment to assay the effect of
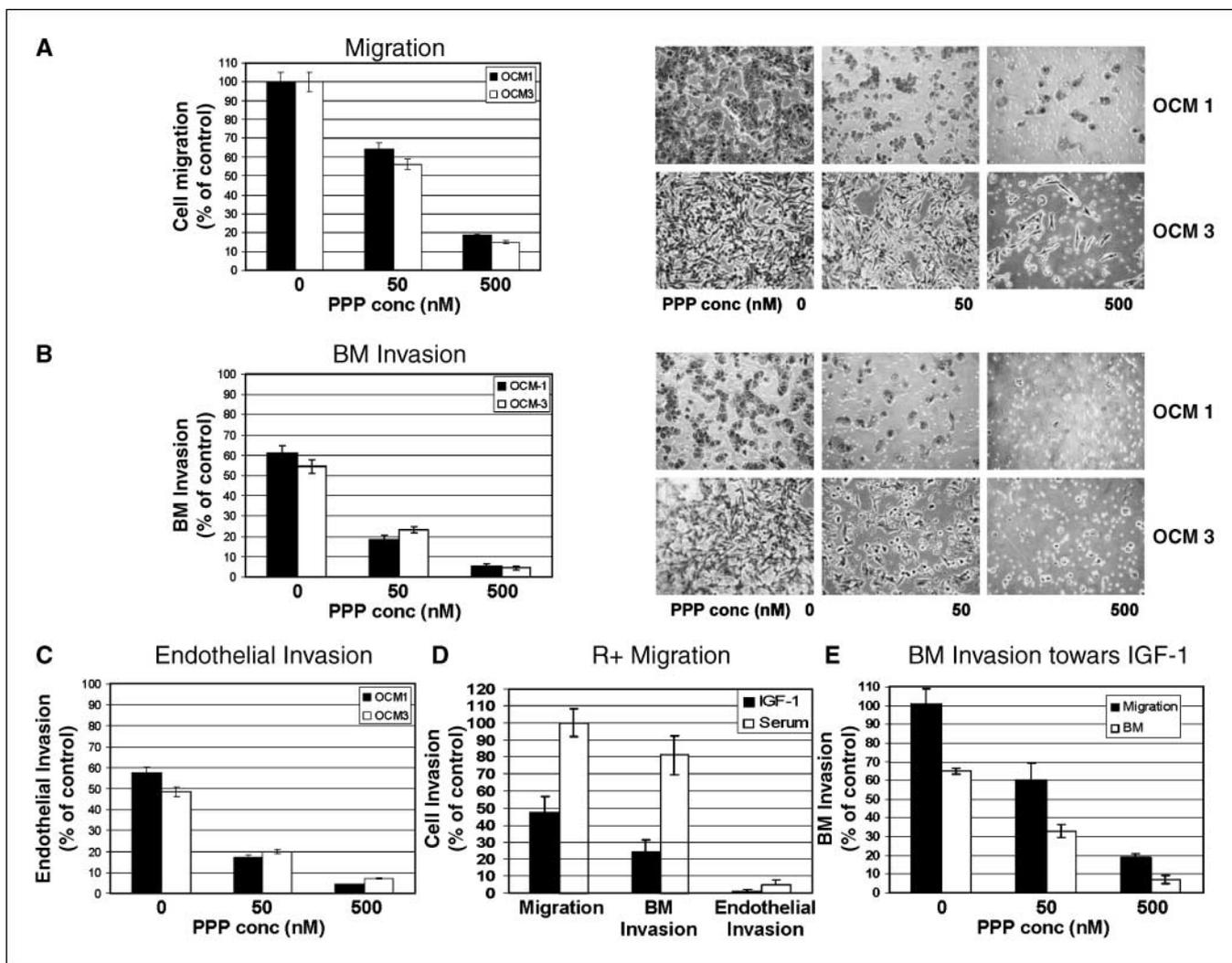
Fig. 3. Effect of PPP on cell migration and invasion. BD BioCoat Matrigel chambers were used to investigate the effect of PPP (50 or 500 nmol/L) on cell migration (*A*), basement membrane (*B*), and endothelial invasion (*C*) of OCM-1 and OCM-3 cells using 10% serum as a chemoattractant. *A* and *B*, right, microphotographs of cells that have passed the membrane and reached the chamber bottom. Cells were treated with PPP (0, 50, or 500 nmol/L) for 1 hour, carefully washed, and then incubated in the Matrigel chambers overnight. All obtained results (number of passing cells) in (*A-C*) are related to the number of cells passing through the membrane without basement membrane or endothelial cells. Results are therefore expressed as % of control. Columns, mean of six experiments; bars, SD. ***, $P < 0.005$; ****, $P < 0.001$. *D*, R+ cells (mouse fibroblasts overexpressing IGF-IR) were incubated overnight in the BD BioCoat Matrigel chambers to investigate migration, basement membrane, and endothelial invasion. Either IGF-I (100 ng/mL) or 10% serum was used a chemoattractant. The obtained values are expressed as percentages of migration values of cells attracted by 10% serum. *E*, effect of PPP on migration and basement membrane invasion of OCM-1 cells using IGF-I (100 ng/mL) in serum-free medium instead of 10% serum as a chemoattractant. Columns, mean of three experiments; bars, SD.
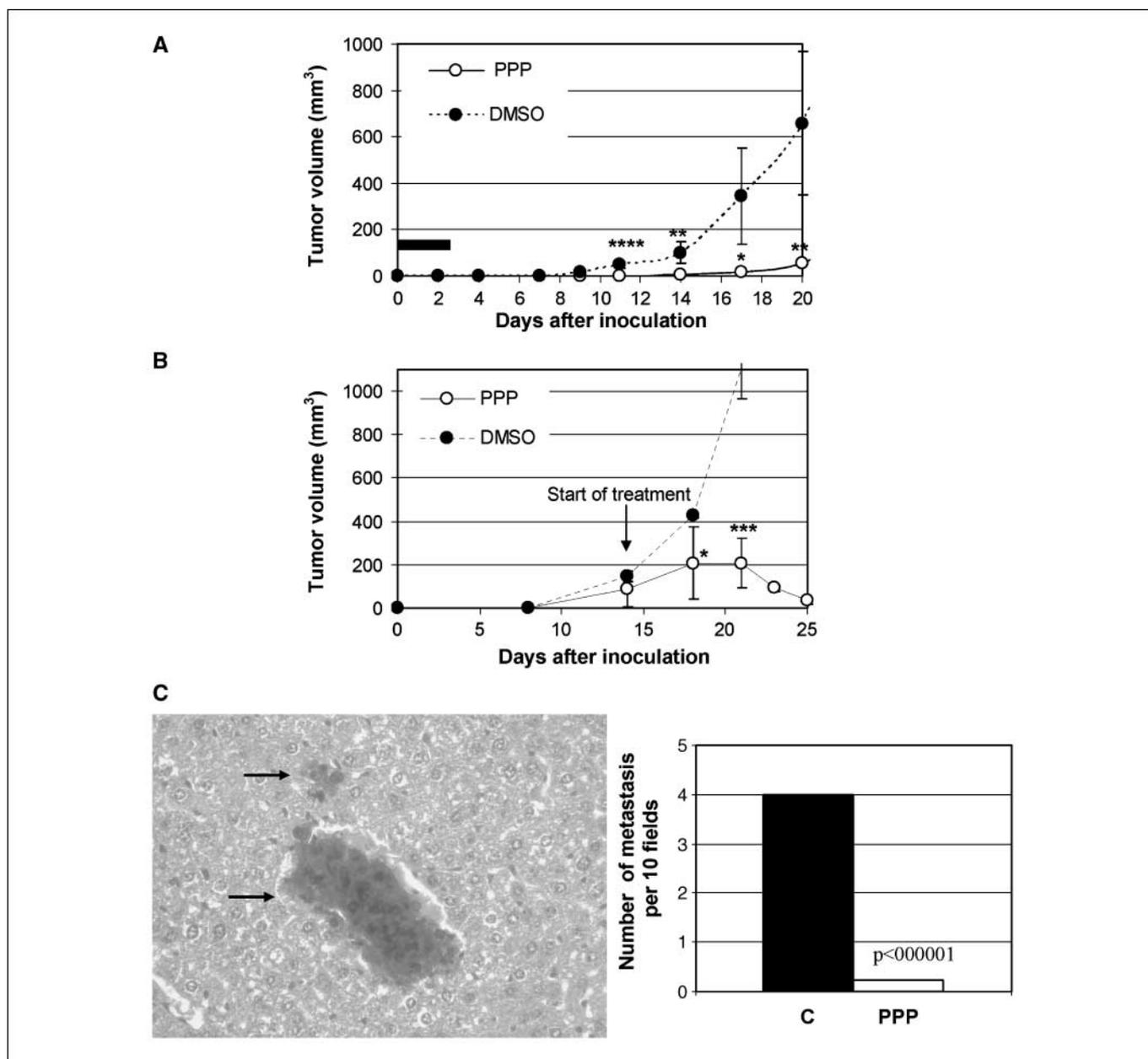
Fig. 4. Effects of PPP on uveal melanoma establishment, growth, and micrometastases in mice. *A,* OCM-1 cells were injected s.c. in severe combined immunodeficient mice (day 0). The mice were treated with PPP (20 mg/kg) or drug-free solvent (DMSO) i.p. twice a day on days 0, 1, and 2. The experiment was terminated at day 20. Points, mean of tumor sizes; bars, SD. *, $P < 0.05$; **, $P < 0.01$; ****, $P < 0.001$. *B,* OCM-1 cells were injected s.c. in severe combined immunodeficient mice. When the tumors had been established and reached sizes of 100 to 350 mm^3, mice were treated with PPP or drug-free solvent i.p. twice a day for 12 days. Tumor sizes were measured regularly. Points, mean; bars, SD. *, $P < 0.05$; ***, $P < 0.005$. *C,* liver tissues from control and PPP-treated mice were prepared for histology. Left, histology of liver tissue from a mouse in the control group; arrows, melanoma micometastases. Right, number of liver micrometastases per 10 high-power fields (200×) in control mice and PPP-treated mice. Columns, mean; bars, SD.

PPP on basement membrane invasion. Of the control cells, 55% to 60% could pass the basement membrane after an overnight incubation, but if the cells had been treated with PPP for 1 hour only, 20% and 5% of the cells could invade through the basement membrane depending on the PPP concentration (50 and 500 nmol/L, respectively; Fig. 3B). Finally, the reconstituted basement membrane was covered by confluent endothelial cells to assay the invasive ability of uveal melanoma cells on this barrier. Using this *in vitro* model, the capability of tumor cells to invade through vessel endothelium can be evaluated. As shown in Fig. 3C, the addition of endothelial

barrier decreased the invasive capability of the untreated uveal melanoma cells only marginally compared with the basement membrane barrier (cf. Fig. 3B), indicating that the tumor cells can easily pass through the endothelial cell layer. The inhibitory effect of PPP on the endothelial invasion was of the same magnitude as that on the basement membrane invasion. As a control experiment to examine quality of the endothelial layer, we investigated the ability of nontumorigenic cells to cross the endothelial cell/basement membrane combination. When serum was used as a chemoattractant, these cells (R+) exhibited 100% migration and 80% of them could pass the basement

membrane barrier but failed to invade through the endothelial cell/basement membrane combination (Fig. 3D). However, when IGF-I was used as a chemoattractant, ~45% of the cells migrated and <20% invaded the basement membrane but no cells could invade the endothelial layer (Fig. 3D). We also investigated the effects of PPP on migration and basement membrane invasion of cells exposed to IGF-I as a chemo-attractant. The experiment was done on OCM-1 cells. As shown, IGF-I caused 100% migration and ~60% invasion

through the basement membrane barrier (Fig. 3E). PPP resulted in a dose-dependent decrease in both variables, similar to that seen in cells attracted by serum (cf. Fig. 3A and B).

Effects of PPP on uveal melanoma xenografts. As shown in Fig. 1B, PPP efficiently reduced survival of cultured uveal melanoma cells. Next, we investigated the effects of PPP on establishment and growth of uveal melanoma *in vivo*. OCM-1 cell xenografts were produced s.c. in severe combined immunodeficient mice. This cell line, which has been reported
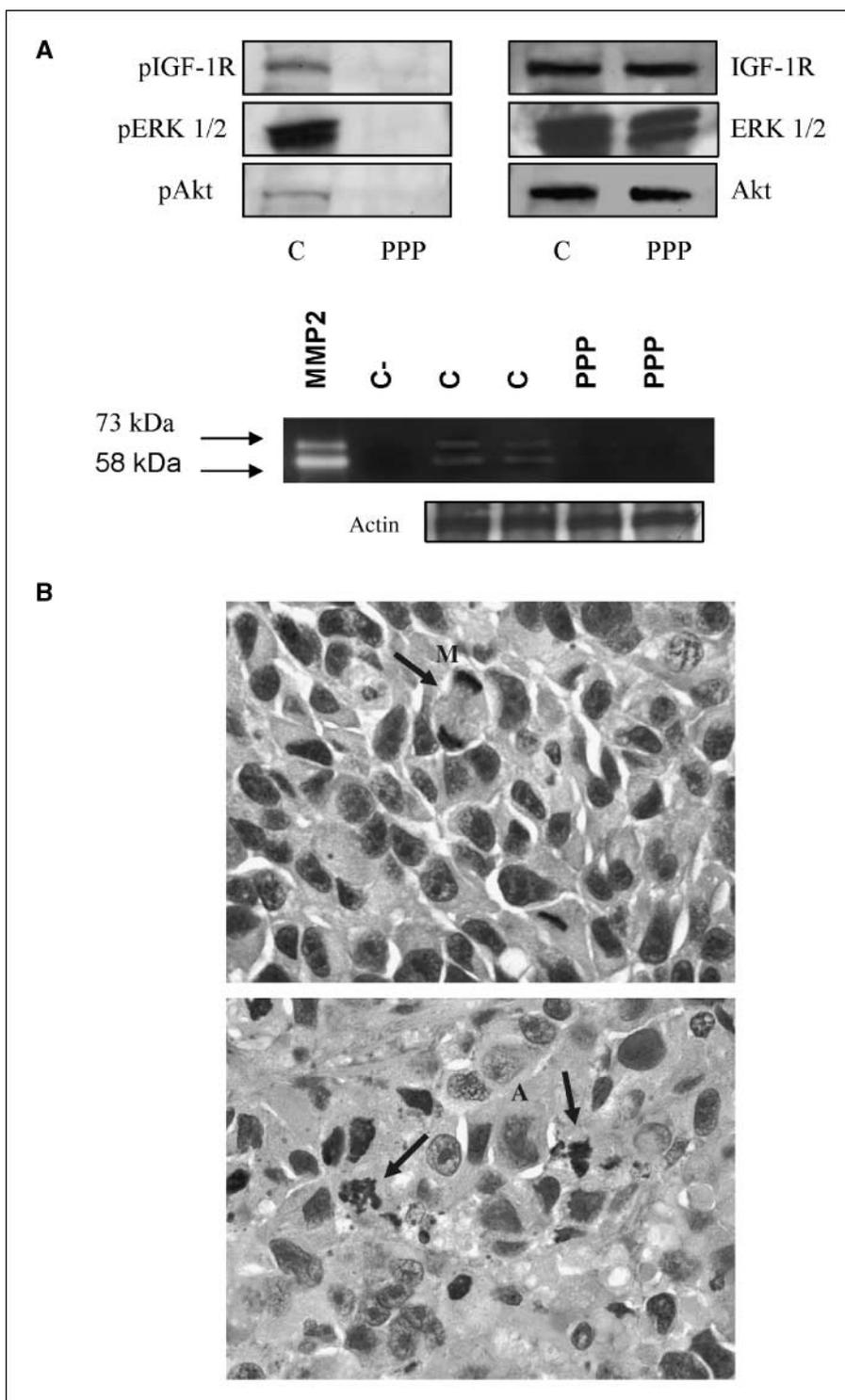
Fig. 5. Effects of PPP on phosphorylation of IGF-IR, Akt, and ERK1/2 as well as on MMP-2 activity and apoptotic rate. *A,* in a separate experiment, established OCM-1-xenografted mice were treated with DMSO (control) and PPP (20 mg/kg/12 h) for 4 days. From the tumor samples, protein lysates were prepared and analyzed for expression of phosphorylated IGF-IR, Akt, and ERKs as well for gelatinolytic activity of MMP-2. *B,* separate samples were prepared for histologic sections. In the control section, two typical mitoses are indicated by M. In PPP-treated tumor, several apoptotic cells are seen and indicated by A.

to be tumorigenic elsewhere (29), established well in 2 weeks (Fig. 4A). One group of mice, after inoculation, was directly treated with PPP for 3 days; after which, they were kept untreated until the experiment was stopped after additional 17 days. Figure 4A shows clearly detectable tumors in control (DMSO) mice after 11 days and in the PPP-treated ones after 20 days. At this time, the tumor volumes measured 658 and 54 mm^3 (in average) in DMSO- and PPP-treated mice, respectively. Thus, this early short PPP treatment dramatically reduced tumorigenesis of uveal melanoma cells. We also investigated the effects of PPP on already established tumors. The tumors exhibited sizes of 100 to 150 mm^3 at this time and grew steadily. The mice were treated with PPP for 12 days. As shown in Fig. 4B, the tumors immediately responded with growth inhibition and, after 7 days, they started regressing drastically. The mice did not exhibit any weight loss or other side effects during the treatment period. Similar results were also obtained in xenografts established from OCM-3 and 92-1 cells (data not shown). In a parallel experiment on established tumors treated with DMSO and PPP for 12 days, we investigated the presence of micrometastases in liver in the two groups. Figure 4C (*left*) shows the histology of liver tissues from a control mouse. Micrometastases can easily be detected. In samples from PPP-treated mice, extremely few tumor cell aggregates were visible in the liver. Figure 4C (*right*) shows the highly significant decrease in incidence of micrometastases in the PPP group of mice.

In a parallel experiment, mice with established tumors were treated with DMSO or PPP only for 4 days (before regression started; cf. Fig. 4B). Some tumor samples were snap-frozen for analysis of phosphorylation of IGF-IR, Akt, and ERK1/2 as well as for assay of MMP-2 gelatinolytic activity. Other samples were fixed in formalin for preparation of histologic sections. Figure 5A shows that treatment with PPP caused strong inhibition of IGF-IR, Akt, and ERK1/2 phosphorylation in tumor tissues. Moreover, expression of MMP-2 was decreased. Figure 4B shows histology of tumor samples. As compared with the control tumors (from mice treated with DMSO), those from PPP-treated mice exhibited a lot of apoptotic figures (Fig. 4B). Analysis of the number of apoptotic cells from several sections shows a strongly significant increase in samples isolated from PPP-treated mice compared with DMSO-treated ones (Table 1).

Table 1. PPP induces apoptosis in uveal melanoma *in vivo*

Treatment*	No. apoptotic cells/10 high-power fields (mean ± SD)[†]	Significance[‡]
DMSO	22.3 ± 1.6	—
PPP	63.7 ± 4.1	$P < 0.001$

*OCM-1-xenografted mice treated with DMSO and PPP (20 mg/kg/12h) for 4 days.
[†]Histologic sections were prepared from tumors and analyzed for numbers of apoptotic cells per 10 high power fields (200×). Means and SDs from 10 sections are shown.
[‡]Significance levels were determined by Students *t* test.

Discussion

This study shows that the IGF-IR inhibitor PPP efficiently decreases survival of cultured uveal melanoma cells and causes regression of uveal melanoma tumor xenografts in mice. Moreover, PPP strongly attenuates several mechanisms involved in invasion (cell adhesion to ECM proteins, MMP-2 expression and activity, cell migration, and basement membrane and endothelial invasion) as well as reduces implantation and establishment of uveal melanoma cells. Because both invasion and tumor cell establishment comprise crucial events in metastasis, our findings raise the possibility of applying IGF-IR inhibitors as adjuvants or neoadjuvants in therapeutic management of uveal melanoma patients.

The invasive progression of tumors is a major impediment for successful treatment of neoplastic diseases in general (30) and of uveal melanoma in particular (1, 2). Today, up to 50% of the patients with operated primary uveal melanoma develop metastases and, unfortunately, most of them succumb to the disease.

Usually, ECM constitutes the first barrier against tumor spread. The term vascular mimicry describes the unique ability of highly aggressive uveal melanoma cells to form matrix-rich networks, mimicking embryonic vasculogenesis (31). Hess et al. (32) have recently suggested that the phosphoinositol-3-kinase pathway promotes vascular mimicry by regulating the activity of MMP-2 and cleavage of the laminin 5-2 chain. Interestingly, the IGF-IR signaling pathway, through the phosphoinositol-3-kinase branch, has been shown to play important roles in the interaction with ECM. IGF-IR has been found to control cell migration and integrin-mediated adhesion to ECM proteins (26). IGF-IR may influence adhesion to ECM proteins in several ways. It may affect expression of integrins and may also cause activation of specific integrins (26, 33). In this context, focal adhesion kinase, shown to be regulated by IGF-IR through the phosphoinositol-3-kinase/Akt pathway (26, 33), probably is involved.

Further, IGF-IR has been shown to affect biosynthesis and activation of MMPs (22, 34). These findings are consistent with our present results showing that inhibition of IGF-IR, using PPP, significantly decreases uveal melanoma cell adhesion to the ECM proteins fibronectin, laminin, and collagen IV, as well as down-regulates the expression and activity of MMP-2. We could also prove that MMP-2 expression is down-regulated in tumors *in vivo*.

The next crucial step in metastasis is the tumor cell adherence to, and digestion of, the basement membrane to enable passage into the blood stream. The main components of basement membrane are laminin and collagen IV. Both the adherence of tumor cells to the basement membrane and MMP-2-mediated basement membrane digestion have been shown to be under the control of IGF-IR (34). Using the Matrigel model, we found that PPP strongly inhibits the basement membrane invasion of uveal melanoma cells.

A third important step in metastasis is establishment of circulating tumor cells in a new tissue. This step can experimentally be investigated by determining the ability of tumor cells to produce tumors in immunosuppressive animals. We found that early short treatments with PPP drastically delayed tumor formation. This result is consistent with other studies showing

that the IGF-IR is important for production of metastatic tumors (34, 35). Most importantly, we could show in the current study that the incidence of micrometastases in the liver of uveal melanoma xenografted mice was drastically reduced.

In conclusion, our study provides further support for an important role of IGF-IR in uveal melanoma and raises the possibility of using IGF-IR inhibitors in treatment of ongoing disease as well as in prevention of development of metastases.

References

1. Rajpal S, Moore R, Karakousis CP. Survival in metastatic ocular melanoma. Cancer 1983;52:334–6.

2. Diener-West M, Hawkins BS, Markowitz JA, Schachat AP. A review of mortality from choroidal melanoma. II. A meta-analysis of 5-year mortality rates following enucleation, 1966 through 1988. Arch Ophthalmol 1992;110:245–50.

3. Stetler-Stevenson WG, Aznavoorian S, Liotta LA. Tumor cell interactions with the extracellular matrix during invasion and metastasis. Annu Rev Cell Biol 1993;9:541–73.

4. Baker JK, Elshaw SR, Mathewman GE, et al. Expression of integrins, degradative enzymes and their inhibitors in uveal melanoma: differences between *in vitro* and *in vivo* expression. Melanoma Res 2001;11:265–73.

5. Yu H, Rohan T. Role of the insulin-like growth factor family in cancer development and progression. J Natl Cancer Inst 2000;92:1472–89.

6. Baserga R. The insulin-like growth factor I receptor: a key to tumor growth? Cancer Res 1995;55:249–52.

7. LeRoith D, Werner H, Beitner-Johnson D, Roberts CT, Jr. Molecular and cellular aspects of the insulin-like growth factor I receptor. Endocr Rev 1995;16:143–63.

8. Larsson O, Girnita A, Girnita L. Role of insulin-like growth factor 1 receptor signalling in cancer. Br J Cancer 2005;92:2097–101.

9. Zhang H, Yee D. The therapeutic potential of agents targeting the type I insulin-like growth factor receptor. Expert Opin Investig Drugs 2004;13:1569–77.

10. Yakar S, Leroith D, Brodt P. The role of the growth hormone/insulin-like growth factor axis in tumor growth and progression: lessons from animal models. Cytokine Growth Factor Rev 2005;16:407–20.

11. Bhoumik A, Gangi L, Ronai Z. Inhibition of melanoma growth and metastasis by ATF2-derived peptides. Cancer Res 2004;64:8222–30.

12. Hsu MY, Meier F, Herlyn M. Melanoma development and progression: a conspiracy between tumor and host. Differentiation 2002;70:522–36.

13. All-Ericsson C, Girnita L, Seregard S, Bartolazzi A, Jager MJ, Larsson O. Insulin-like growth factor-1 receptor in uveal melanoma: a predictor for metastatic disease and a potential therapeutic target. Invest Ophthalmol Vis Sci 2002;43:1–8.

14. Girnita A, Girnita L, del Prete F, Bartolazzi A, Larsson O, Axelson M. Cyclolignans as inhibitors of the insulin-like growth factor-1 receptor and malignant cell growth. Cancer Res 2004;64:236–42.

15. Vasilcanu D, Girnita A, Girnita L, Vasilcanu R, Axelson M, Larsson O. The cyclolignan PPP induces activation loop-specific inhibition of tyrosine phosphorylation of the insulin-like growth factor-1 receptor. Link to the phosphatidyl inositol-3 kinase/Akt apoptotic pathway. Oncogene 2004;23:7854–62.

16. Stromberg T, Ekman S, Girnita L, et al. IGF-1 receptor tyrosine kinase inhibition by the cyclolignan PPP induces G_2/M-phase accumulation and apoptosis in multiple myeloma cells. Blood 2006;107:669–78.

17. Menu E, Jernberg Wiklund H, Stromberg T, et al. Inhibiting the IGF-1 receptor tyrosine kinase with the cyclolignan PPP: an *in vitro* and *in vivo* study in the 5T33MM mouse model. Blood 2006;107:655–60.

18. Ulfarsson E, Karstrom A, Yin S, et al. Expression and growth dependency of the insulin-like growth factor I receptor in craniopharyngioma cells: a novel therapeutic approach. Clin Cancer Res 2005;11:4674–80.

19. Girnita L, Girnita A, Larsson O. Mdm2-dependent ubiquitination and degradation of the insulin-like growth factor 1 receptor. Proc Natl Acad Sci U S A 2003;100:8247–52.

20. Girnita L, Girnita A, Brodin B, et al. Increased expression of insulin-like growth factor I receptor in malignant cells expressing aberrant p53: functional impact. Cancer Res 2000;60:5278–83.

21. Girnita L, Shenoy SK, Sehat B, et al. β-Arrestin is crucial for ubiquitination and down-regulation of the insulin-like growth factor-1 receptor by acting as adaptor for the MDM2 E3 ligase. J Biol Chem 2005;280:24412–9.

22. Zhang D, Bar-Eli M, Meloche S, Brodt P. Dual regulation of MMP-2 expression by the type 1 insulin-like growth factor receptor: the phosphatidylinositol 3-kinase/Akt and Raf/ERK pathways transmit opposing signals. J Biol Chem 2004;279:19683–90.

23. Qiang YW, Yao L, Tosato G, Rudikoff S. Insulin-like growth factor I induces migration and invasion of human multiple myeloma cells. Blood 2004;103:301–8.

24. Woodward JK, Rennie IG, Elshaw SR, Burn JL, Sisley K. Invasive and noninvasive uveal melanomas have different adhesive properties. Eye 2005;19:342–8.

25. Berube M, Talbot M, Collin C, et al. Role of the extracellular matrix proteins in the resistance of SP6.5 uveal melanoma cells toward cisplatin. Int J Oncol 2005;26:405–13.

26. Leventhal PS, Feldman EL. Insulin-like growth factors as regulators of cell motility—signaling mechanisms. Trends Endocrinol Metab 1997;8:1–6.

27. Albini A, Iwamoto Y, Kleinman HK, et al. A rapid *in vitro* assay for quantitating the invasive potential of tumor cells. Cancer Res 1987;47:3239–45.

28. Sato H, Takino T, Okada Y, et al. A matrix metalloproteinase expressed on the surface of invasive tumour cells. Nature 1994;370:61–5.

29. Kan-Mitchell J, Mitchell MS, Rao N, Liggett PE. Characterization of uveal melanoma cell lines that grow as xenografts in rabbit eyes. Invest Ophthalmol Vis Sci 1989;30:829–34.

30. Rasmussen HS, McCann PP. Matrix metalloproteinase inhibition as a novel anticancer strategy: a review with special focus on batimastat and marimastat. Pharmacol Ther 1997;75:69–75.

31. Maniotis AJ, Folberg R, Hess A, et al. Vascular channel formation by human melanoma cells *in vivo* and *in vitro*: vasculogenic mimicry. Am J Pathol 1999;155:739–52.

32. Hess AR, Seftor EA, Seftor RE, Hendrix MJ. Phosphoinositide 3-kinase regulates membrane Type 1-matrix metalloproteinase (MMP) and MMP-2 activity during melanoma cell vasculogenic mimicry. Cancer Res 2003;63:4757–62.

33. Felding-Habermann B. Integrin adhesion receptors in tumor metastasis. Clin Exp Metastasis 2003;20:203–13.

34. Zhang D, Samani AA, Brodt P. The role of the IGF-I receptor in the regulation of matrix metalloproteinases, tumor invasion and metastasis. Horm Metab Res 2003;35:802–8.

35. Lopez T, Hanahan D. Elevated levels of IGF-1 receptor convey invasive and metastatic capability in a mouse model of pancreatic islet tumorigenesis. Cancer Cell 2002;1:339–53.

The insulin-like growth factor-I receptor inhibitor picropodophyllin causes tumor regression and attenuates mechanisms involved in invasion of uveal melanoma cells.

Ada Girnita, Charlotta All-Ericsson, Mario A Economou, et al.

Updated version	Access the most recent version of this article at: http://clincancerres.aacrjournals.org/content/12/4/1383

Cited articles	This article cites 35 articles, 15 of which you can access for free at: http://clincancerres.aacrjournals.org/content/12/4/1383.full#ref-list-1
Citing articles	This article has been cited by 16 HighWire-hosted articles. Access the articles at: http://clincancerres.aacrjournals.org/content/12/4/1383.full#related-urls

E-mail alerts	Sign up to receive free email-alerts related to this article or journal.
Reprints and Subscriptions	To order reprints of this article or to subscribe to the journal, contact the AACR Publications Department at pubs@aacr.org.
Permissions	To request permission to re-use all or part of this article, use this link http://clincancerres.aacrjournals.org/content/12/4/1383. Click on "Request Permissions" which will take you to the Copyright Clearance Center's (CCC) Rightslink site.